COMPDYN 2015
5th ECCOMAS Thematic Conference on
Computational Methods in Structural Dynamics and Earthquake Engineering
M. Papadrakakis, V. Papadopoulos, V. Plevris (eds.)
Crete Island, Greece, 25–27 May 2015

INTERNAL PARAMETRIC RESONANCE AND AEROELASTIC EFFECTS FOR LONG-SPAN SUSPENSION BRIDGES

Raffaele Ardito[1], Antonio Capsoni[2], and Andrea Guerrieri[1,2]

[1] Dept. of Civil and Environmental Engineering, Politecnico di Milano
Piazza Leonardo da Vinci 32, Milan, Italy
raffaele.ardito@polimi.it

[2] Dept. of Architecture, Built Environment and Construction Engineering, Politecnico di Milano
Piazza Leonardo da Vinci 32, Milan, Italy
antonio.capsoni@polimi.it, andrea.guerrieri@mail.polimi.it

Keywords: Suspension Bridges, Non-linear Dynamics, Aeroelasticity, Stability, Parametric Resonance, Floquet Theory.

Abstract. *The potential occurrence of internal parametric resonance phenomena has been recently indicated as a possible cause of failure for long-span suspension bridges. At the same time, suspension bridges, in view of their flexibility, are prone to aeroelasticity driven response, such as vortex shedding, torsional divergence and flutter. In this paper, a non-linear dynamic model of a suspension bridge is devised, with the purpose of providing a unified framework for the study of aeroelastic and internal resonance instabilities. Inspired by the pioneering work of Herrmann and Hauger, the analyses have been based on a linearized formulation that is able to represent the main structural non-linear effects and the coupling given by aerodynamic forces. The results confirm that the interaction between aeroelastic effects and non-linear internal resonance leads to unstable phenomena for wind speeds which are by far lower than the critical threshold for standard aeroelasticity.*

1 INTRODUCTION

The emergence of new materials and advanced structural engineering technology makes suspension bridges a spontaneous answer for demands of larger spans, light weight, high strength, ease of construction, and aesthetic appearance. On one hand, the flexibility caused by the cable system and its long span makes the suspension bridges sensitive to dynamic loads; on the other hand, the relatively simple geometry of cable structures makes continuum approaches still very attractive, since can be based on a minimal number of non-dimensional parameters.
Early attempts on static equilibrium of suspension bridge were made by Moisseiff, who extended the elastic theory to the well-established Deflection Theory [1,2] by enforcing equilibrium in the deformed position, and accounting for the stiffening effect in the main cables. Earliest continuum models for the linear vertical vibrations of suspension bridges reproduced the effects of the stiffening truss girder by means of an Euler–Bernoulli beam supported by the main cables through inextensible and distributed vertical hangers. In this regard, the classic continuum model for the linear vertical vibration of suspension bridges, based on the so called linearized deflection theory, was first proposed by Bleich et al. [3], and Steinman [4], which derived some formulas for computing natural frequencies and mode shapes, and recently reviewed by Luco and Turmo [5]. The last authors showed that the linear vibration of the considered suspension bridge model is completely governed by two non-dimensional parameters: the classic Irvine parameter of suspended cables, first introduced by Irvine [6] and a second parameter accounting for the relative stiffness of the girder with respect to the main cable system. Abdel-Ghaffar in the late 1970's [7-9] developed the methodology of free vertical, torsional and lateral vibration analysis of suspension bridges by means of a variational principle and a finite element approach. Then, the same author [10-12] extended the continuum formulation to include coupling between vertical–torsional vibrations, nonlinear effects occurring in the case of large vibrations and the effects of distortional deformation of the girder cross-section.
Nowadays, in the design of suspension bridges a comprehensive set of wind related responses are taken into consideration, such as static divergence, vortex-shedding, buffeting and flutter. Hence, the risk of developing aeroelastic instabilities is always the matter while designing any lightweight long-span structures, characterized by high flexibility due to a low bending/torsional stiffness and a high width-to-depth ratio. Although the phenomenon was already well known in aviation, the research on flutter in civil engineering field started as the collapse of the Tacoma Narrows Bridge (USA) in 1940, when the catastrophe was seen mainly as a direct consequence of flutter [13] that developed on the bridge deck at wind speed much lower than the design one. Flutter is generally studied within linearized aeroelastic models, which can provide the range of wind speeds where Hopf bifurcation occurs. To consider the effects due to the unsteadiness of the relative motion between the section and the air flow, indicial Theodorsen type [14,15] formulations can be adopted to predict more accurately the critical wind speed at the onset of the flutter instability [16] with respect to the quasi-steady formulation. The equations of motion for suspension bridges were employed for aeroelastic investigations in [17], where analysis are centered on experimentally determined flutter derivatives, and a full three-dimensional modal analysis of the structure.
It's well known from non-linear dynamics that, between coupled oscillators, energy transfer [18] can occur as far as the energetic levels reaches critical well established thresholds. Classically this behaviour is referred to as the *internal resonance* phenomenon. Many authors applied this principles to study the vibrations response of suspension bridges. The authors of [19,20] used the continuous model proposed by Abdel-Ghaffar [11], and solve the system of

equations by means of the multiple scale perturbative technique [21]. Recently, Airoli and Gazzola [22], trying to explain why did torsional oscillations suddenly appears before the Tacoma Narrows collapse, found out that also in isolated systems as vertical oscillations become large enough they may switch to torsional ones. The problem was already tackled by other authors [23-27] but no one was able to identify the actual causes of that sudden large torsional oscillations. Hence, they paved the way for future works concerning the interaction between internal resonance and aeroelastic phenomena, as the present paper wants to do.
The article intends to study the stability of a suspension bridge model using the continuum formulation proposed by Abdel-Ghaffar in [11] enriched by the terms coming from Theodorsen [15] indicial formulation for the wind-structure interaction. The stability will be checked in Lyapunov asymptotic sense exploiting the well-known Floquet theory [28]. The varational system of equations is obtained following the procedure proposed by Herrman [29] assuming small but finite flexural perturbations coming from vortex-shedding excitation. The possibility of parametric internal resonances such as harmonic, sub-harmonic and super-harmonic, or additive combinational and anti-resonances will be checked by means of suitable stability maps.
Section 2 starts with a brief review of the parametric modal analysis for the continuum suspension bridge model [11] focusing on the so called cross over frequencies already proposed in [5] for the only flexural oscillations, and here extended to the torsional component. In Section 3, the aerodynamic additional mass, stiffness and damping are introduce in the original model by means of the analytical formulation [30] for the so called Flutter derivatives. Section 3 is devoted to the linearized variational system of equations projected in the modal space. The analysis of stability maps confirm the possibility of parametric resonance of 2:1 type between flexural and torsional motion already verified by other authors [11,19,20] by means of analytical procedure but on the complete non-linear original system of equations. The importance of bridge's deck sectional shape factor will be stressed out in order to explain Parametric resonance phenomenon by means of Strohual linear law for vortex-shedding excitation. Conclusions will be delegate to Section 4.

2 STRUCTURAL PROBLEM FORMULATION

A continuum model of single span, linearly elastic, suspension bridge is considered (Fig. 1). The bridge, having a span length *l*, is composed by two main cables that support the stiffening girder (bridge deck) through uniformly distributed, massless and inextensible vertical hangers. The main cables are hinged at fixed anchors placed at the same vertical elevation and are modeled as mono-dimensional continua with negligible flexural, torsional and shear rigidities. The stiffening girder is modeled as an equivalent, uniform, Euler-Bernoulli beam, with flexural hinges and torsional forks at its ends. The distortional deformation of the cross-section is neglected. The cross-section of the girder has double symmetry with respect to vertical and horizontal local axes, y and z respectively (Fig. 1). The contribution of the stiffening girder in carrying dead loads is disregarded: dead loads are entirely carried by the main cables and are assumed to be uniformly distributed along the longitudinal axis.

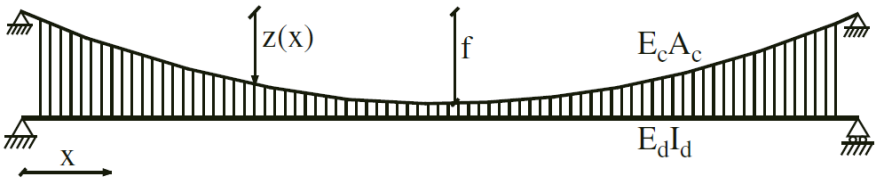

Figure 1: Single span suspension bridge model

2.1 Nonlinear coupled equations of motion

The motion of the bridge is described by means of three generalized displacement functions (Fig. 2): vertical deflection $w_d(x,t)$, twist rotation $\theta_d(x,t)$ about the longitudinal centerline of the deck-cables system and warping displacement $u_d(x,t)$ of the cross-section, t denoting time. The equations of motion are derived by means of Hamilton's principle $\delta\left\{\int_{t_1}^{t_2}(T-V+W)dt\right\}=0$, where $\delta\{\cdot\}$ is the variational operator, T and V are the total kinetic and potential energies of the system, respectively, W is the work done by external forces and t_1 and t_2 are arbitrary time instants.

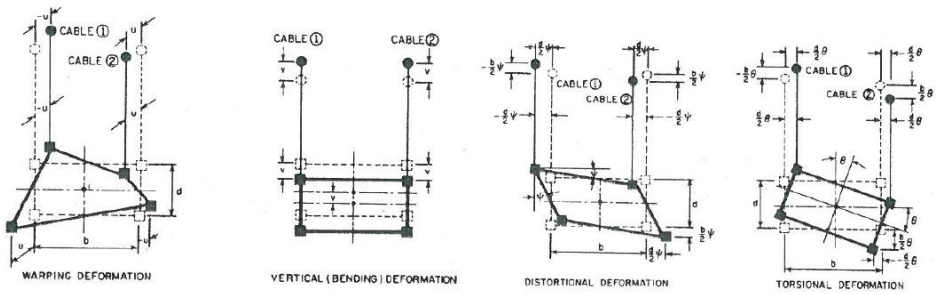

Figure 2: Four principal different kinds of displacements

The development of Hamilton's equation yields the non-linear coupled equations of motion of the suspension bridge with the associated boundary conditions. Detailed calculations are omitted for the sake of brevity. After some manipulations, the following dimensionless equations are obtained. Notice that the equations are written separating the linear from the quadratic and cubic parts on different rows.

$$\frac{d^2\tilde{w}_d}{d\tau^2}+\mu^2\cdot\tilde{w}_d{}'^{v}-\tilde{w}_d{}''+\lambda_L{}^2\tilde{h}_w+$$

$$flexural\ :\quad -\lambda_Q{}^2\cdot\left[\tilde{h}_w\cdot\tilde{w}_d{}''+\tilde{h}_\vartheta\cdot\tilde{\vartheta}_d{}''-\frac{1}{2}\left(\tilde{h}_{w'w'}+\tilde{h}_{\vartheta'\vartheta'}\right)\right]+\quad=\tilde{q}(\xi,\tau)\qquad(1)$$

$$\left\lfloor\quad -\lambda_C{}^2\cdot\left[\frac{1}{2}\left(\tilde{h}_{w'w'}+\tilde{h}_{\vartheta'\vartheta'}\right)\cdot\tilde{w}_d{}''+\tilde{h}_{w'\vartheta'}\cdot\tilde{\vartheta}_d{}''\right]\quad\right\rfloor$$

$$\tilde{J}_t\cdot\frac{d^2\tilde{\vartheta}_d}{dt^2}+\frac{\beta^2}{\chi^2}\cdot\tilde{\vartheta}_d{}'^{v}-(1+\beta^2)\cdot\tilde{\vartheta}_d{}''+\lambda_L{}^2\tilde{h}_\vartheta+$$

$$\text{torsional}\ :\qquad -\lambda_Q{}^2\cdot\left[\tilde{h}_\vartheta\cdot\tilde{w}_d{}''+\tilde{h}_w\cdot\tilde{\vartheta}_d{}''-\tilde{h}_{w'\vartheta'}\right]+\qquad=\tilde{m}(\xi,\tau)\qquad(2)$$

$$\left\lfloor-\lambda_C{}^2\cdot\left[\tilde{h}_{w'\vartheta'}\cdot\tilde{w}_d{}''+\frac{1}{2}\left(\tilde{h}_{w'w'}+\tilde{h}_{\vartheta'\vartheta'}\right)\cdot\tilde{\vartheta}_d{}''\right]\right\rfloor$$

The following non-dimensional parameters have been introduced.

$$\begin{array}{lll} \xi = \frac{x}{l} & {\lambda_L}^2 = \frac{E_c A_c}{H}\frac{l}{L_c}(y''l)^2 = & \widetilde{J_t} = \frac{(J_t + 2m_c b^2)}{(m_d + 2m_c)\cdot b^2} \\ & = 8{\lambda_Q}^2 = 64{\lambda_C}^2 & \\ \tau = t \cdot \frac{1}{l}\sqrt{\frac{2H}{(m_d+2m_c)}} & \mu^2 = \frac{E_d I_d}{2Hl^2} & \tilde{h}_{ij} = \int_0^1 i \cdot j \, d\xi \\ \widetilde{w}_d(\xi,\tau) = \frac{w_d(x,t)}{f} & \chi^2 = \frac{G_d J_d l^2}{E_d \Gamma_d} & \tilde{q}(\xi,\tau) = \frac{l^2}{2Hf} q(\xi,\tau) \\ \begin{cases} \tilde{\vartheta}_d(\xi,\tau) = \frac{\vartheta_d(x,t)\cdot b}{f} \end{cases} & \begin{cases} \beta^2 = \frac{G_d J_d}{2Hb^2} \end{cases} & \begin{cases} \widetilde{m}(\xi,\tau) = \frac{l^2}{2Hfb} m(\xi,\tau) \end{cases} \end{array} \tag{3}$$

where x is the bridge axis coordinate, l the main span length, t the time variable, H the initial cables tension, m_d and m_c respectively the deck and single cable mass per unit length, $w_d(x,t)$ and $\vartheta_d(x,t)$ respectively the flexural and torsional motion of the of the deck axis, f the initial cables sag, and b the half width of the deck section.

The Irvine parameter ${\lambda_L}^2$ of the main cables [6], which is crucial in determining the eigen-properties of the bridge, depends also upon the axial stiffness of the cables system $E_c A_c$, the cables initial length L_c and the initial cables curvature assumed by the parabolic shape $y'' = 8f/l^2$. Notice that the assumption of initial parabolic shape of the main cables allows us to define in a simple form the quadratic and cubic Irvine terms.

Other relevant non-dimensional parameters are μ^2 (Steinman's stiffness factor [2]) and β^2, that reflect the relative flexural and torsional rigidities of the girder, respectively. They depends upon the deck flexural $E_d I_d$ and the primary (St. Venant) torsional $G_d J_d$ stiffness. Moreover, in order to account for the warping deformability of the section we need to introduce the so called warping coefficient reflecting the ratio between the primary and secondary $E_d \Gamma_d$ (Vlasov-Wagner) torsional stiffness.

We can define a dimensionless equivalent torsional inertia per unit length dependent both on the cables and deck contribution J_t. The so called stiffening operator $\tilde{h}_{ij}$ synthetize in different terms the stiffness contribution coming from the main cables tension increment (stiffening behavior). Finally we need to introduce some dimensionless external forces normalizing the generalized vertical force $q(\xi,\tau)$ and torsional couple $m(\xi,\tau)$ acting on the bridge deck axis.

2.2 Linear free vibrations

A solution of the equations of motion is sought with the following general modal expansion form.

$$\widetilde{w}_d(\xi,\tau) = \sum_{n=1}^{\infty} W_n(\xi) \cdot \left\{ Z_n \cdot \exp\left(i \cdot \widetilde{\omega}_{w,n} \cdot \tau\right) + c.c. \right\} \quad with \;\; n \in \aleph \backslash \{0\} \tag{4}$$

$$\tilde{\vartheta}_d(\xi,\tau) = \sum_{m=1}^{\infty} \Theta_m(\xi) \cdot \left\{ \Gamma_m \cdot exp\left(i \cdot \widetilde{\omega}_{\vartheta,m} \cdot \tau\right) + c.c. \right\} \quad with \;\; m \in \aleph \backslash \{0\} \tag{5}$$

Being the general dimensionless circular frequency defined as :

$$\widetilde{\omega}_{(\cdot)} = \omega_{(\cdot)} \cdot l \sqrt{\frac{(m_d + 2m_c)}{2H}} \tag{6}$$

By enforcing the suitable boundary conditions for the flexural hinges $\{\widetilde{w}_d(0,\tau) = \widetilde{w}_d(1,\tau) = 0 \; ; \; \widetilde{w}_d{}''(0,\tau) = \widetilde{w}_d{}''(1,\tau) = 0\}$ and for the torsional forks $\{\tilde{\vartheta}_d(0,\tau) = \tilde{\vartheta}_d(1,\tau) = 0 \; ; \; \tilde{\vartheta}_d{}''(0,\tau) = \tilde{\vartheta}_d{}''(1,\tau) = 0\}$, one obtains the natural frequencies and the symmetric and anti-symmetric modes. get the following symmetric modal shape expressions. It is worth noting

that the former include trigonometric and hyperbolic functions, conversely the latter are represented by simple sinusoidal shapes.

The influence of the main parameters ${\lambda_L}^2$, χ^2, μ^2, and β^2 has been investigated through a parametric analysis, based on the available data collected from literature [5,12,31-40]. Besides realistic values also extreme situations are considered such as ${\lambda_L}^2 = 0$ (flat cables), ${\lambda_L}^2 = \infty$ (inextensible cables), $\mu^2 = 0$ (flexible deck), $\chi^2 = 0$ (rigid warping), $\chi^2 = \infty$ (free warping), $\beta^2 = 0$ (flexible deck).

For the sake of brevity, we will report just the results obtained for the second mode of vibrations, that shows more interesting features than the first one. Figure 3 shows the flexural eigenfrequency, as a function of the dimensionless deck bending stiffness, for different values of the Irvine parameter. Figure 4 is referred to torsional eigenfrequency, in the case of free warping.

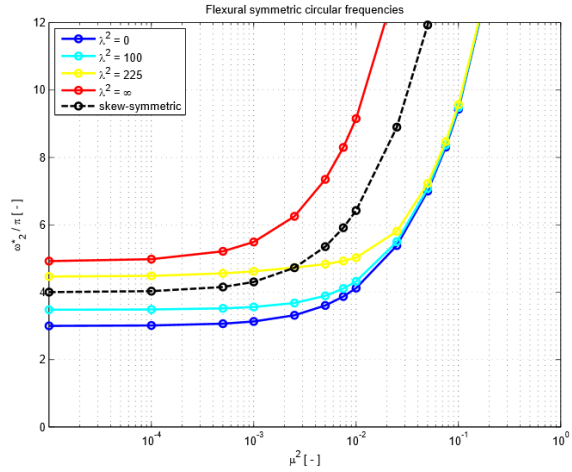

Figure 3: Circular eigen-frequencies of flexural symmetric mode 2.

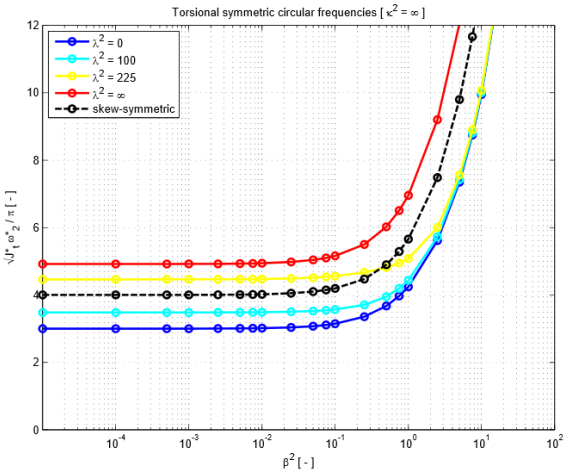

Figure 4: Circular eigen-frequencies of torsional symmetric mode 2 for $\chi^2 = \infty$.

The modal shapes associated to previously analyzed frequencies are very similar for flexural and torsional vibrations (Figures 5 and 6). The upward (negative) displacement increases as the Irvine parameter ${\lambda_L}^2$ does, since as cables become more and more inextensible, their initial parabolic shape turns out to be much more influent on deck deformation. As ${\lambda_L}^2 = \infty$, the modal shapes coalesce approximately to a single sinusoidal curve for any value of μ^2 and β^2. Similarly, if higher modes are considered ($n > 4$), one gets modal shapes closer to sinusoidal ones since the hyperbolic cosine contribution becomes negligible, meaning that deck stiffness is less influent on bridge vibration. Notice that increasing the relative deck stiffness (flexural and torsional) the positive antinodal points move away from the midspan. Concerning torsional modes only, passing from $\chi^2 = \infty$ to $\chi^2 = 0$ we noticed that the deck relative stiffness becomes much more relevant in the latter case.

2.3 Cross over frequencies and modes

As previously mentioned frequencies and modal shapes associate to higher order modes features interesting behavior. First, we want to focus the attention on the so-called [5] Cross Over Frequency (COF), that is the frequency common to symmetric and skew-symmetric modes. As this particular condition occurs, symmetric modal shapes will vibrate according to frequencies proper of skew-symmetric ones. In order to reach the COF threshold condition the structural parameters of the suspension bridge has to be properly tuned (as shown in Figures 3 and 4).

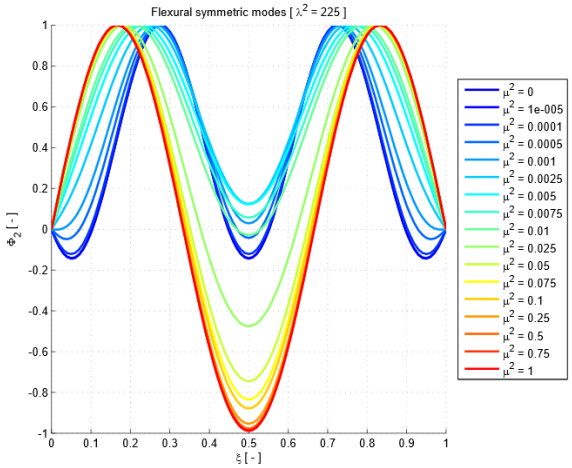

Figure 5: Modal shape of flexural mode 2 for ${\lambda_L}^2 = 225$.

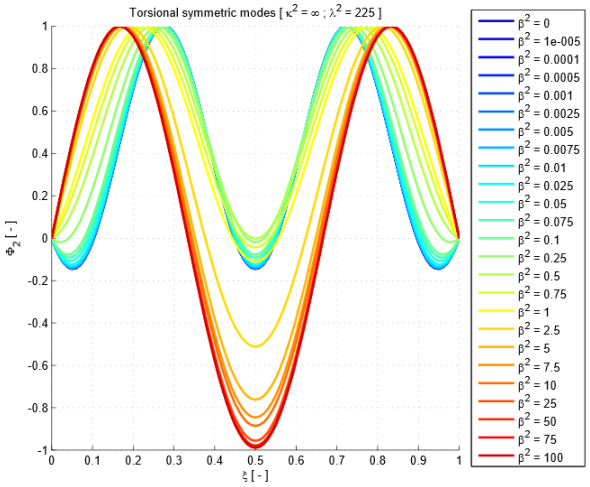

Figure 6: Modal shape of torsional mode 2 for ${\lambda_L}^2 = 225$ and $\chi^2 = \infty$.

As can be seen from Figures 5-6, the modal shapes are strongly influenced by the structural parameters of the suspension bridges. In the design process, it can be useful to tune some parameters in order to improve the bridge performance, such as in regard of edge slope and peak upward motion. Enforcing the vanishing of the latter two parameters, we get critical conditions for the modal shapes, that, by analogy with the previous treatment, we can be referred to as Cross Over Modes (COM). Concerning the COM conditions we can state that only the first symmetric modes has a unique critical curve: in fact, as the edge slopes vanish the peak upward displacement does the same.

3 AEROELASTIC ANALYSIS

For sake of simplicity, the wind-structure interaction has been modelled by means of Theodorsen Theory that consider a thin airfoil immersed in a uniform and constant potential air stream. The main advantage is that the formulation will be independent from the actual sectional shape of the bridge's deck. Though we are implicitly modelling the deck by means of a thin plate, the inaccuracy introduced by the modelling could be comparable to numerical approximations typical of finite elements discretization.

3.1 Theodorsen formulation

Let's write the aerodynamic lift and couple acting on the axis of the bridge's deck.

$$L(t) = \pi b^2 \rho_a \cdot \ddot{w}_d + 2\pi b \rho_a U \cdot \left\{ C_w \cdot \dot{w}_d + \frac{b}{2}(1 + C_\theta) \cdot \dot{\theta}_d \right\} + 2\pi b \rho_a U^2 C_\theta \cdot \theta_d \qquad (7)$$

$$M(t) = -\frac{\pi}{8} b^4 \rho_a \cdot \ddot{\vartheta}_d + \pi b^2 \rho_a U \cdot \left\{ C_w \cdot \dot{w}_d + \frac{b}{2}(1 - C_\theta) \cdot \dot{\theta}_d \right\} + \pi b^2 \rho_a U^2 C_\theta \cdot \theta_d \qquad (8)$$

Where we have used the air density $\rho_a \cong 1.18\, kg/m^3$, the mean wind speed U and the so-called Theodorsen complex functions, that notice, being dependent on the actual reduced frequency $\tilde{k}_{(\cdot)}$, are different for the flexural C_w and the torsional motion C_θ.

$$C_{(\cdot)} = C\left(\tilde{k}_{(\cdot)}\right) = F\left(\tilde{k}_{(\cdot)}\right) + i \cdot G\left(\tilde{k}_{(\cdot)}\right) \qquad (9)$$

$$\tilde{k}_{(\cdot)} = \omega_{(\cdot)} \frac{b}{U} \qquad (10)$$

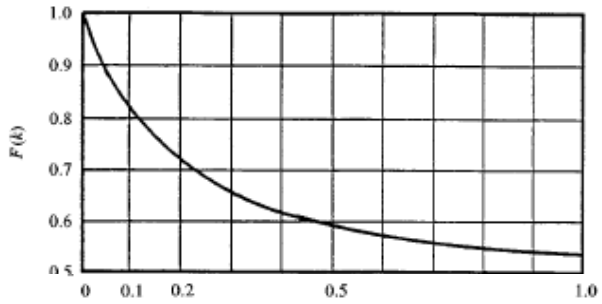

Figure 7: Real part of Theodorsen complex function.

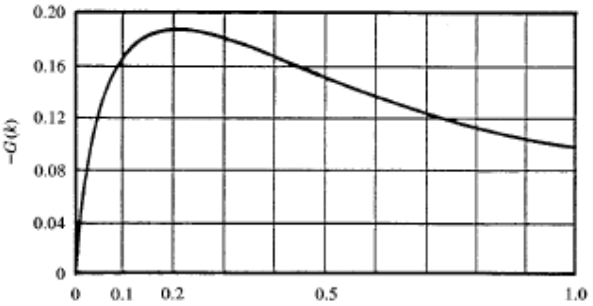

Figure 8: Imaginary part of Theodorsen complex function.

3.2 Linear coupled equations on motion

Before proceeding, we stress the fact that aeroelastic forces introduces additional linear terms only. Hence, also the linear equations of motion becomes coupled and the system loses its symmetries in stiffness and damping, thus becoming susceptible of static divergence and flutter dynamic instability. The dimensionless linear coupled equations of motion reads:

$$\frac{d^2\tilde{w}_d}{d\tau^2} + \tilde{c}_{ww} \cdot \frac{d\tilde{w}_d}{d\tau} + \tilde{c}_{w\vartheta} \cdot \frac{d\tilde{\vartheta}_d}{d\tau} + \mu^2 \cdot \tilde{w}_d{}'^{v} - \tilde{w}_d{}'' + \lambda_L{}^2 \tilde{h}_w + 2\tilde{k}_{\vartheta\vartheta} \cdot \theta_d = 0 \qquad (11)$$

$$\widetilde{J_t} \cdot \frac{d^2\tilde{\vartheta}_d}{d\tau^2} + \tilde{c}_{\vartheta\vartheta} \cdot \frac{d\tilde{\vartheta}_d}{d\tau} + \tilde{c}_{\vartheta w} \cdot \frac{d\tilde{w}_d}{d\tau} + \frac{\beta^2}{\chi^2} \cdot \tilde{\vartheta}_d{}'^{v} - (1+\beta^2) \cdot \tilde{\vartheta}_d{}'' - \tilde{k}_{\vartheta\vartheta} \cdot \theta_d + \lambda_L{}^2 \tilde{h}_\vartheta = 0 \qquad (12)$$

In the above equations, we have neglected the additional mass $\widetilde{m}_a$ and torsional inertia $\widetilde{J_a}$ coming from the participating air mass. In fact from the available data [5,12,31-40] it turns out that they are always negligible contributions with respect to structural ones.
The following definitions hold.

$$\tilde{c}_{ww} = 2\left(\xi_w \cdot \tilde{\omega}_w + \sqrt{\widetilde{J_t} \cdot \widetilde{m}_a} \cdot \tilde{\Omega}_\vartheta \cdot \tilde{u} \cdot C_w\right)$$

$$\tilde{c}_{w\vartheta} = \sqrt{\widetilde{J_t} \cdot \widetilde{m}_a} \cdot \tilde{\Omega}_\vartheta \cdot \tilde{u} \cdot (1 + C_\theta)$$

$$\tilde{c}_{\vartheta\vartheta} = 2\sqrt{\widetilde{J_t}} \cdot \left\{\xi_\vartheta \cdot \sqrt{\widetilde{J_t}} \cdot \tilde{\omega}_\vartheta + \frac{1}{4} \cdot \sqrt{\widetilde{m}_a} \cdot \tilde{\Omega}_\vartheta \cdot \tilde{u} \cdot (1 - C_\theta)\right\} \qquad (13)$$

$$\tilde{c}_{\vartheta w} = -\sqrt{\widetilde{J_t} \cdot \widetilde{m}_a} \cdot \tilde{\Omega}_\vartheta \cdot \tilde{u} \cdot C_w$$

$$\tilde{k}_{\vartheta\vartheta} = \widetilde{J_t} \cdot \tilde{\Omega}_\vartheta{}^2 \cdot \tilde{u}^2 \cdot C_\theta$$

where $\xi_{(\cdot)}$ is the structural equivalent viscous damping ratio, assumed for simplicity constant and equal to 0.5%, whilst $\tilde{u}$ represent the mean wind speed U normalized with respect to the static divergence one U_D in correspondence of the same structural parameters.

$$U_D = \sqrt{\widetilde{J_t} \cdot \tilde{\Omega}_\vartheta{}^2} \cdot \sqrt{\frac{2H}{\pi\rho_a l^2}} \qquad (14)$$

Notice the difference between $\tilde{\Omega}_{(\cdot)}$ and $\tilde{\omega}_{(\cdot)}$, which represent, respectively, the circular frequency obtained from the undamped structural model and the one coming from the complete aeroelastic analysis. Consequently, the first will be constant and the second will vary as the mean wind speed does.
Lastly, the generic dimensionless reduced frequencies can be defined as follows.

$$\tilde{k}_{(\cdot)} = \left(\tilde{\omega}_{(\cdot)} - i\tilde{\alpha}_{(\cdot)}\right) \cdot \sqrt{\tilde{m}_a} / \left(\sqrt{\tilde{J}_t} \cdot \tilde{\Omega}_\vartheta \cdot \tilde{u}\right) \tag{15}$$

The linearized equation, considered in this Section, is of basic importance in order to obtain the wind speed which corresponds to flutter onset. In fact, having obtained a modal projection of the governing equations, one can enforce the flutter conditions by considering a null value for torsional or flexural damping. Figure 9 shows an example of computation: for the specific structural parameters, torsional flutter happens in correspondence of the wind speed marked by a red circle.

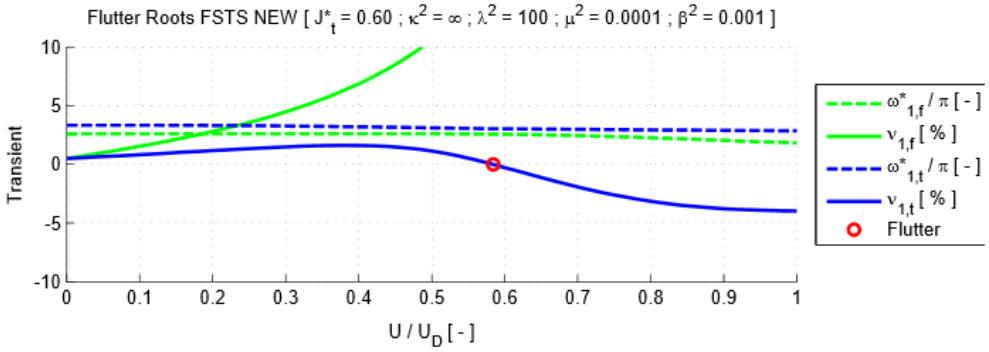

Figure 9 Variation of flexural and torsional frequencies and damping ratios with wind speed level.

4 INTERNAL PARAMETRIC RESONANCE

The recent work by Airoli and Gazzola [22] and previous works by different authors [19,20] contain the numerical and analytical proof, respectively, that suspension bridges can suffer of internal parametric resonance. This kind of phenomenon strongly differs from the well-known ordinary resonance characteristic of linear vibrating systems. The main differences lie in the fact that, regarding the parametric resonance, no external sources of energy are a priori needed since energy is just transferred from one mode to another.

4.1 Modal projection of nonlinear aeroelastic equations

In order to catch the internal resonance phenomenon, it is necessary to consider the fully nonlinear equation of motion, supplemented by the aeroelastic terms considered in Section 3. By applying a modal projection of the governing equations, based on generic (rather than exponential) time-varying functions, one finds:

$$\begin{aligned} &M_{w,n} \cdot \ddot{z}_n + C_{w,n} \cdot \dot{z}_n + C_{w\vartheta,nm} \cdot \dot{\gamma}_m + K_{w,n}^{(L)} \cdot z_n + K_{w\vartheta,nm}^{(L)} \cdot \gamma_m + \\ &+K_{w,n}^{(Q)} \cdot {z_n}^2 + K_{w\vartheta,nm}^{(Q)} \cdot {\gamma_m}^2 + \\ &\left(+K_{w,n}^{(C)} \cdot {z_n}^3 + K_{w\vartheta,nm}^{(C)} \cdot z_n \cdot {\gamma_m}^2 \right) \end{aligned} = \Gamma_{w,n} \tag{16}$$

$$\begin{aligned} &J_{\vartheta,m} \cdot \ddot{\gamma}_m + C_{\vartheta,m} \cdot \dot{\gamma}_m + C_{\vartheta w,mn} \cdot \dot{z}_n + K_{\vartheta,m}^{(L)} \cdot \gamma_m + \\ &+K_{\vartheta w,mn}^{(Q)} \cdot \gamma_m \cdot z_n + \\ &\left(+K_{\vartheta,m}^{(C)} \cdot {\gamma_m}^3 + K_{\vartheta w,mn}^{(C)} \cdot \gamma_m \cdot {z_n}^2 \right) \end{aligned} = \Gamma_{\vartheta,m}(\xi,\tau) \tag{17}$$

The following equivalent masses, damping, stiffness and forcing terms have been introduced.

$$M_{w,n} = \int_0^1 {W_n}^2(\xi)d\xi; \quad C_{w,n} = \tilde{c}_{ww} \cdot M_{w,n}; \quad C_{w\vartheta,nm} = \tilde{c}_{w\vartheta} \cdot \tilde{h}_{W_n,\Theta_m} \tag{18}$$

$$K_{w,n}^{(L)} = \int_0^1 W_n(\xi) \cdot [\mu^2 \cdot {W_n}^{IV}(\xi) - {W_n}''(\xi)]d\xi + {\lambda_L}^2 \cdot \tilde{h}_{{W_n}^2}; \quad K_{w\vartheta,nm}^{(L)} = 2\tilde{k}_{\vartheta\vartheta} \cdot \tilde{h}_{W_n,\Theta_m} \tag{19}$$

$$K_{w,n}^{(Q)} = \frac{3}{2} \cdot {\lambda_Q}^2 \cdot \tilde{h}_{W_n} \cdot \tilde{h}_{W_n'^2}; \quad K_{w\vartheta,nm}^{(Q)} = {\lambda_Q}^2 \cdot \left\{\tilde{h}_{\Theta_m} \cdot \tilde{h}_{W_n',\Theta_m'} + \frac{1}{2} \cdot \tilde{h}_{W_n} \cdot \tilde{h}_{\Theta_m'^2}\right\} \tag{20}$$

$$K_{w,n}^{(C)} = \frac{1}{2} \cdot {\lambda_C}^2 \cdot \left(\tilde{h}_{W_n'^2}\right)^2; \quad K_{w\vartheta,nm}^{(C)} = {\lambda_C}^2 \cdot \left\{\frac{1}{2} \cdot \tilde{h}_{\Theta_m'^2} \cdot \tilde{h}_{W_n'^2} + \left(\tilde{h}_{W_n',\Theta_m'}\right)^2\right\} \tag{21}$$

$$M_{\vartheta,m} = \int_0^1 {\Theta_m}^2(\xi)d\xi \Rightarrow J_{\vartheta,m} = \widetilde{J_t} \cdot M_{\vartheta,m} \tag{22}$$

$$C_{\vartheta,m} = \tilde{c}_{\vartheta\vartheta} \cdot M_{\vartheta,m}; \quad C_{\vartheta w,mn} = \tilde{c}_{\vartheta w} \cdot \tilde{h}_{W_n,\Theta_m} \tag{23}$$

$$K_{\vartheta,m}^{(L)} = \int_0^1 \Theta_m(\xi) \cdot \left[\frac{\beta^2}{\chi^2} \cdot {\Theta_m}^{IV}(\xi) - (1+\beta^2) \cdot {\Theta_m}''(\xi)\right] d\xi + {\lambda_L}^2 \cdot \tilde{h}_{{\Theta_m}^2} - \tilde{k}_{\vartheta\vartheta} \cdot M_{\vartheta,m} \tag{24}$$

$$K_{\vartheta w,mn}^{(Q)} = {\lambda_Q}^2 \cdot \begin{Bmatrix} 2 \cdot \tilde{h}_{\Theta_m} \cdot \tilde{h}_{W_n',\Theta_m'} + \\ \\ +\tilde{h}_{W_n} \cdot \tilde{h}_{\Theta_m'^2} \end{Bmatrix} \tag{25}$$

$$K_{\vartheta,m}^{(C)} = {\lambda_C}^2 \cdot \left(\tilde{h}_{\Theta_m'^2}\right)^2; \quad K_{\vartheta w,mn}^{(C)} = {\lambda_C}^2 \cdot \left\{\left(\tilde{h}_{W_n',\Theta_m'}\right)^2 + \frac{1}{2} \cdot \tilde{h}_{W_n'^2} \cdot \tilde{h}_{\Theta_m'^2}\right\} \tag{26}$$

$$\Gamma_{\vartheta,m} = \int_0^1 \Theta_m(\xi) \cdot \tilde{m}(\xi,\tau)d\xi \tag{27}$$

It is important to notice that in the torsional equation of motion it is not possible to define a second order term independently from the flexural component. This is because the rotations of the deck introduces an asymmetric response of the two main cables, which strongly depend on the flexural amplitude of vibration affecting the stiffness of the cables system. This property of the system will be fundamental in the following in order to study the stability of vibrations.

4.2 Vortex-shedding modelling

In many real-life systems, mainly in the electrical field, the parameters which govern the equations of motion may vary periodically in time [41]. When dealing with suspension bridges, this is not the case since structural parameters are fixed and can vary only in a very long period. Nevertheless, in view of the peculiar non-linear coupling of the governing equations and accounting for the presence of aeroelastic phenomena, one can easily realize that parametric resonance may occur in suspension bridge in the presence of a periodic external action. This may happen even if the wind velocity remains constant, because of the vortex-shedding phenomenon. It is well known that, under certain conditions, vortex detaches from the immersed body in a regular and periodic variation in time and space. This condition is the so-called Von Kármán vortex street phenomenon, that has been verified experimentally to occur in circular cylinders in a range of Reynolds number of about $250 < Re < 2 \cdot 10^5$.
In the case of bridges, vortex-shedding effect can be represented by means of a sinusoidal transverse force:

$$F_L = \frac{1}{2} \cdot \rho_a \cdot B \cdot U^2 \cdot C_L \cdot \sin(\omega_{VS} \cdot t) \tag{28}$$

where ω_{VS} is the frequency of vortex shedding and C_L is the lift coefficient, which basically depends on the cross section shape, on the Reynolds number and on the surface roughness. The equivalent modal lift force has the following dimensionless format.

$$\Gamma_{w,n} = \Gamma_0 \cdot \tilde{h}_{W_n} \cdot \sin(\tilde{\omega}_{VS} \cdot \tau) \tag{29}$$

$$\Gamma_0 = \tilde{B} \cdot \tilde{c}_L \cdot \tilde{J}_t \cdot \tilde{\Omega}_{\vartheta,m}{}^2 \cdot \tilde{u}^2 \tag{30}$$

where we have introduced the non-dimensional counterpart for the deck's width and the normalized lift coefficient with respect to the analytical one characterizing thin airfoils.

$$\tilde{B} = B/f = 0.17 \div 0.51 \cong 0.32 \tag{31}$$

$$\tilde{c}_L = C_L(\theta_d)/2\pi \tag{32}$$

It is worth noting that the stability analyses will be carried out by considering the forcing frequency as an independent variable. When examining the results, it will be necessary to account for the well-known Strouhal relationship, which connects the vortex shedding frequency to the mean wind speed:

$$\omega_{VS} = 2\pi \cdot f = 2\pi \cdot St \cdot U/D \tag{33}$$

Moreover, the presence of the lock-in region will be accounted for, by considering an interval of wind velocity in which there is a synchronism between structural and vortex shedding frequency. The dimensionless format of Strouhal relationship reads:

$$\tilde{\omega}_{St} = \pi \cdot St \cdot \left(\tilde{\alpha}/\sqrt{\tilde{m}_a}\right) \cdot \sqrt{\tilde{J}_t} \cdot \tilde{\Omega}_{\vartheta,m} \cdot \tilde{u} \tag{34}$$

where $\tilde{\alpha} = B/D$ is the aspect ratio of the cross section: from avalable bridges data [5,12,31-40] $\tilde{\alpha} = 3 \div 12$. Concerning the Strouhal number St, we will make reference to numerical investigations of [43]: it seems reasonable to consider $St \cong 0.1$.
Finally, we must remember that vortex-shedding is a self-limited phenomenon due to the additional viscous aerodynamic damping. By experimental investigations, it is known that oscillations of circular cylinders never overcome the 20% of the cross flow dimension of the body. Consequently an empirical upper bound for dimensionless vertical vibrations should be taken about equal to 0.01.

4.3 Formulation of perturbed system of equations

In order to study the stability of the suspension bridge vibrations as long as dominant flexural motion occurs, we will make reference to the work of Hermann and Hauger [29].
First, we need to assume small flexural vibrations and negligible torsional ones, allowing us to study the linear equation of motion of a SDOF damped and periodically forced oscillator:

$$z_n(t) < \varepsilon \Rightarrow z_n{}^2(t)\ ;\ z_n{}^3(t)\ \cong 0 \tag{35}$$

$$\gamma_m(t) \cong 0 \Rightarrow \tilde{c}_L = C_L(\theta_d = 0)/2\pi \tag{36}$$

The governing equation reads:

$$M_{w,n} \cdot \ddot{z}_n + C_{w,n} \cdot \dot{z}_n + K_{w,n}^{(L)} \cdot z_n = \Gamma_0 \cdot \tilde{h}_{W_n} \cdot sin(\tilde{\omega}_{St} \cdot \tau) \tag{37}$$

The solution will be given by the superposition of a homogenous solution and a particular steady integral. Since we are looking for unstable solutions, the transient conditions are not of interest. Hence the steady state solution will be driven as usual by the so called complex dynamic amplification factor.

$$z_{n,SS}(t) = z_{n,0} \cdot sin(\tilde{\omega}_{St} \cdot \tau - \varphi) \tag{38}$$

$$z_{n,0} = \Gamma_0 \cdot \tilde{h}_{W_n} \cdot |H(\delta)|/M_{w,n} \tag{39}$$

$$|H(\delta)| = \left\{ {\tilde{\Omega}_{w,n}}^2 \cdot \sqrt{\left(1 - \delta^2 - \left({\tilde{c}_{ww}}^I / \tilde{\Omega}_{w,n}\right) \cdot \delta\right)^2 + \left(\left({\tilde{c}_{ww}}^R / \tilde{\Omega}_{w,n}\right) \cdot \delta\right)^2} \right\}^{-1} \tag{40}$$

$$tg(\varphi) = \left({\tilde{c}_{ww}}^R / \tilde{\Omega}_{w,n}\right) \cdot \delta / \left(1 - \delta^2 - \left({\tilde{c}_{ww}}^I / \tilde{\Omega}_{w,n}\right) \cdot \delta\right) \tag{41}$$

$$\delta = \tilde{\omega}_{St} / \tilde{\Omega}_{w,n} \tag{42}$$

The second step requires to introduce a small perturbation to the actual forced system, in terms of both flexural and torsional DOF:

$$z_n(t) = z_{n,0} \cdot \sin(\tilde{\omega}_{St} \cdot \tau - \varphi) + z_{P,n}(t) \quad with \quad z_{P,n}(t) < \varepsilon \tag{43}$$

$$\gamma_m(t) = \gamma_{P,m}(t) \quad with \quad \gamma_{P,m}(t) < \varepsilon \tag{44}$$

Then, by substituting the above definitions in the complete modal aeroelastic system of equations and by suitable linearization, one gets the so-called Perturbed system.

$$M_{w,n}\ddot{z}_{P,n} + C_{w,n}\dot{z}_{P,n} + C_{w\vartheta,nm}\dot{\gamma}_{P,m} + K_{w,n}^{(L)} z_{P,n} + K_{w\vartheta,nm}^{(L)} \gamma_{P,m} = 0 \tag{45}$$

$$J_{\vartheta,m}\ddot{\gamma}_{P,m} + C_{\vartheta,m}\dot{\gamma}_{P,m} + C_{\vartheta w,mn}\dot{z}_{P,n} + \left\{K_{\vartheta,m}^{(L)} + K_{\vartheta w,mn}^{(Q)} z_{n,0} \sin(\tilde{\omega}_{St}\tau - \varphi)\right\}\gamma_{P,m} = 0 \tag{46}$$

As previously mentioned, the second order term of torsional motion is dependent simultaneously and linearly on both motions while the flexural one depends quadratically on the two independent contributions. This makes possible that a small but not vanishing vertical perturbation influences the torsional response, even in a linearized formulation. This kind of phenomenon can be classified as a Parametric excitation problem. In fact, in the perturbed system there is no forcing term but just a periodically varying structural parameter. The fact that it depends on the actual vortex-shedding excitation is hidden inside the terms $z_{n,0}$ and φ.
We have stressed many times the fact that being a self-limiting phenomenon; vortex shedding is able to induce just small flexural perturbations. However, because their effects on torsional vibrations is amplified by the quadratic coupled modal stiffness $K_{\vartheta w,mn}^{(Q)}$, it will be of basic importance to understand its influence on the system response. Consequently, we can say that in the design process will be useful whether is possible to tune the geometrical and mechanical properties of the suspension bridge in order to minimize that cross stiffness.

4.4 Floquet stability conditions

In the previous section, we ended up with the definition of the perturbation system, that is a system of two ordinary differential equation of second order and with periodic coefficients. The stability of such a system can be easily analyzed by exploiting the well-known Floquet Theorem. It has been proved [28] that solutions of those kind of systems can be written as the product between a periodic function $P(t)$ and an exponential one $M(t)$. Consequently, we get asymptotically stable solutions in Lyapunov sense if the periodic function does not diverge.
To check this, we need first to reduce the perturbed system (45-46) of Hill's equation to an equivalent system of the first order.

$$\dot{\boldsymbol{x}} = \boldsymbol{J} \cdot \boldsymbol{x} \tag{47}$$

The procedure requires a simple change of variables that leads to the following definition of Jacobian matrix J.

$$\boldsymbol{x} = \{z_{P,n} \quad \gamma_{P,m} \quad \dot{z}_{P,n} \quad \dot{\gamma}_{P,m}\}^T \tag{48}$$

$$\boldsymbol{J} = \begin{Bmatrix} 0 & \boldsymbol{I} \\ -\boldsymbol{M}^{-1} \cdot \boldsymbol{K} & -\boldsymbol{M}^{-1} \cdot \boldsymbol{D} \end{Bmatrix} \tag{49}$$

$$\boldsymbol{M} = \begin{Bmatrix} M_{w,n} & 0 \\ 0 & J_{\vartheta,m} \end{Bmatrix} \tag{50}$$

$$\boldsymbol{D} = \begin{Bmatrix} C_{w,n} & C_{w\vartheta,nm} \\ C_{\vartheta w,mn} & C_{\vartheta,m} \end{Bmatrix} \tag{51}$$

$$\boldsymbol{K} = \begin{Bmatrix} K_{w,n}^{(L)} & K_{w\vartheta,nm}^{(L)} \\ 0 & K_{\vartheta,m}^{(L)} + K_{\vartheta w,mn}^{(Q)} \cdot z_{n,0} \cdot \sin(\widetilde{\omega}_{St} \cdot \tau - \varphi) \end{Bmatrix} \tag{52}$$

The so-called monodromy matrix gives us the variation of the solution vector after a period. Hence, in order to compute such a matrix, it is simply necessary to perform a numerical integration of the equivalent first order system over the reference period $T = 2\pi$ assuming a number of initial conditions equal to the number of unknowns. The initial values has to be chosen in such a way that the fundamental matrix of solutions is unitary on the main diagonal at the initial instant. This allows us to define the monodromy matrix as follows.

$$\boldsymbol{C} = \{[\boldsymbol{x}(T)]_{z(0)=1} \quad [\boldsymbol{x}(T)]_{\gamma(0)=1} \quad [\boldsymbol{x}(T)]_{\dot{z}(0)=1} \quad [\boldsymbol{x}(T)]_{\dot{\gamma}(0)=1}\} \tag{53}$$

Finally, in order to check the stability of the system it is necessary that any of the eigenvalues of the Monodromy matrix exceeds the unity, in absolute value.

4.5 Stability maps analysis

In the following, we will comment the numerical results obtained from a parametric analysis of the stability of the perturbed system. Results will be collected inside stability maps that are able to synthetize the main information necessary to distinguish between stable and unstable regions. Each of them, in fact, will be characterized by the circular frequency of vortex shedding Ω_{VS} and by a mean wind speed level U.

Two model will be analyzed. The first, called Structural, accounts for geometrical and mechanical properties of the suspension bridge only. This preliminary analysis is useful in order to check if the non-linearities of the dynamic system are strong enough to find out resonance conditions different from the primary linear one. Hence, in this model the term playing a fundamental role is $K_{\vartheta w,mn}^{(Q)}$ since it's the only one able to couple the equations of motion. In fact all damping and stiffening terms coming from aeroelastic effects will not be taken in account.

In the second, Aeroelastic, model both structural and aerodynamic parameters will be considered. The task of this model is to find out if and under which conditions wind effect on suspension bridges, coupled with parametric resonance, is able to lead the structure to unstable conditions. Results will be of relevance only if the structure reaches those critical conditions in correspondence of a wind speed lower than the flutter one.

In both models we will analyze different resonance conditions besides the linear primary one, such as harmonic, subharmonic and superharmonic of order two for both the flexural and the torsional vibrations, and further additive combinational and anti-resonance type.

$$harmonic \;:\; \Omega_{VS} = \omega_i \tag{54}$$

$$subharmonic \;:\; \Omega_{VS} = 2 \cdot \omega_i \tag{55}$$

$$superharmonic \;:\; \Omega_{VS} = \omega_i / 2 \tag{56}$$

$$combinational\ \ sum \;:\; \Omega_{VS} = \omega_w + \omega_\vartheta \tag{57}$$

$$anti-resonance \;:\; \Omega_{VS} = |\omega_w - \omega_\vartheta| \tag{58}$$

We choose to consider just the second order type of internal resonance since we want to catch just the critical conditions near the classical primary linear resonance.
Let's analyze some numerical results starting from the Structural model.
As we can see, Figure 10, the Structural model is able to catch the main resonance of the system. In fact, besides the primary linear flexural one the system undergoes resonance also as the forcing frequency is near the torsional one. Since the excitation frequency is associated to flexural motion, this kind of phenomenon can be associated to an internal resonance of kind 1:1. Further, the model is able to catch also the so-called 2:1 internal resonance as the flexural motion is characterized by a frequency that doubles the torsional one. On the other hand, the effect of other kind of resonances is less evident.
It is worth noting that the presence of internal resonances reduces drastically the critical wind speed level, that in the case of the simple structural model is represented by the torsional divergence speed. However, it's evident that in this case the vortex-shedding phenomenon does not seem to be able to explain any of the previous unstable conditions. In fact, the linear model proposed by Strouhal never reaches the critical conditions in terms of frequencies and amplitudes (wind speed) that lead the system response to diverge in time.

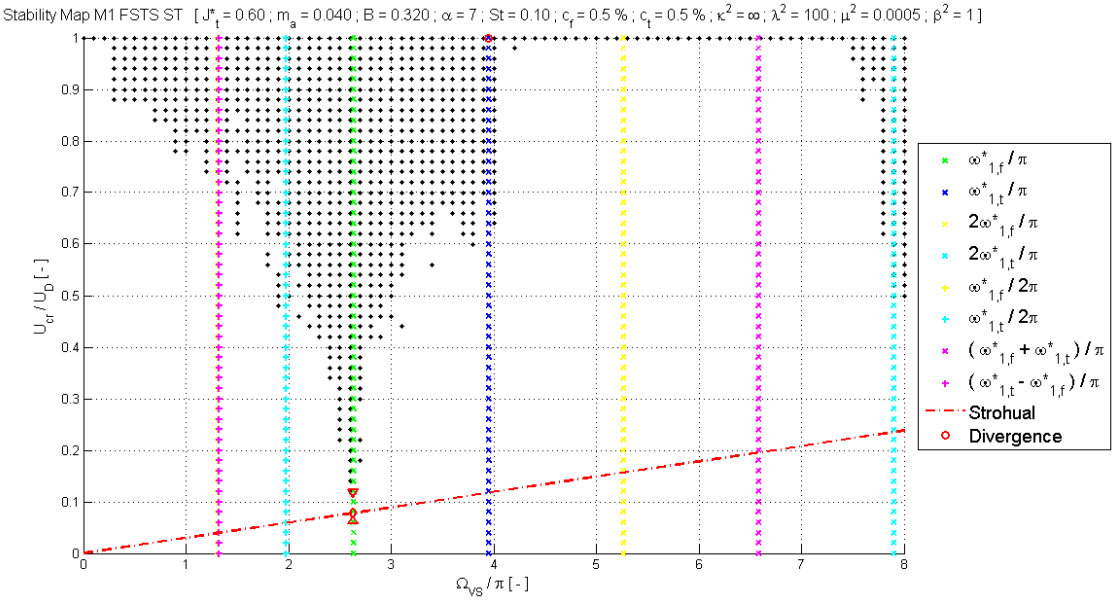

Figure 10: Stability map of the Structural model for slender deck section. The lock-in interval is denoted by a couple of red triangular marks around the critical vortex shedding frequency (red diamond mark).

As already mentioned, in the definition of the dimensionless Strohual circular frequency, a relevant role is played by the deck sectional aspect ratio. In fact, it strongly modifies the slope of the Strohual curve, which consequently can enter the unstable regions. This means that in the design process is fundamental to take in consideration this fact, since the choice of the sectional dimensions of the deck will be of fundamental importance for the dynamic stability of the overall structure.
As we can see in Figure 11, by reducing the aspect ratio down to $\tilde{\alpha} = 3$ the vortex shedding phenomenon is able to explain the main resonant unstable conditions that are the flexural primary linear and the second order subharmonic internal torsional ones.

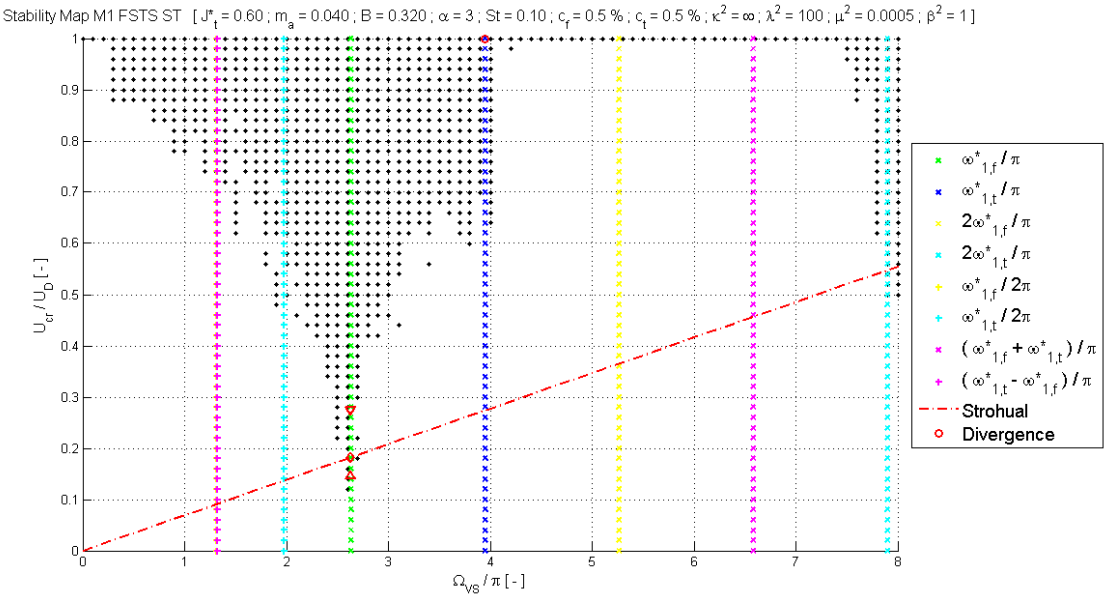

Figure 11: Stability map of the Structural model for bluff deck section.

Hence, we can conclude that very bluff deck sections can be useful to increase torsional and mainly flexural stiffness of the suspension bridge, but they lead the structure to be more susceptible to parametric instabilities due to vortex shedding.

Let's now analyze the Aeroelastic model accounting for the fluid-structure interaction effects on the dynamic stability if the system, Figure 12. As already mentioned in the flutter analysis, the fluid-structure interaction makes the frequencies being dependent on the actual wind speed level, consequently we see curved lines representing the main internal or external resonance conditions. Moreover, the wind-structure interaction enlarges the unstable regions. This is valid also for wind speed which is by far lower than the one required to reach the critical flutter condition. Hence, the interaction between Aeroelasticity and Parametric resonance can lead to unexpected unstable conditions.

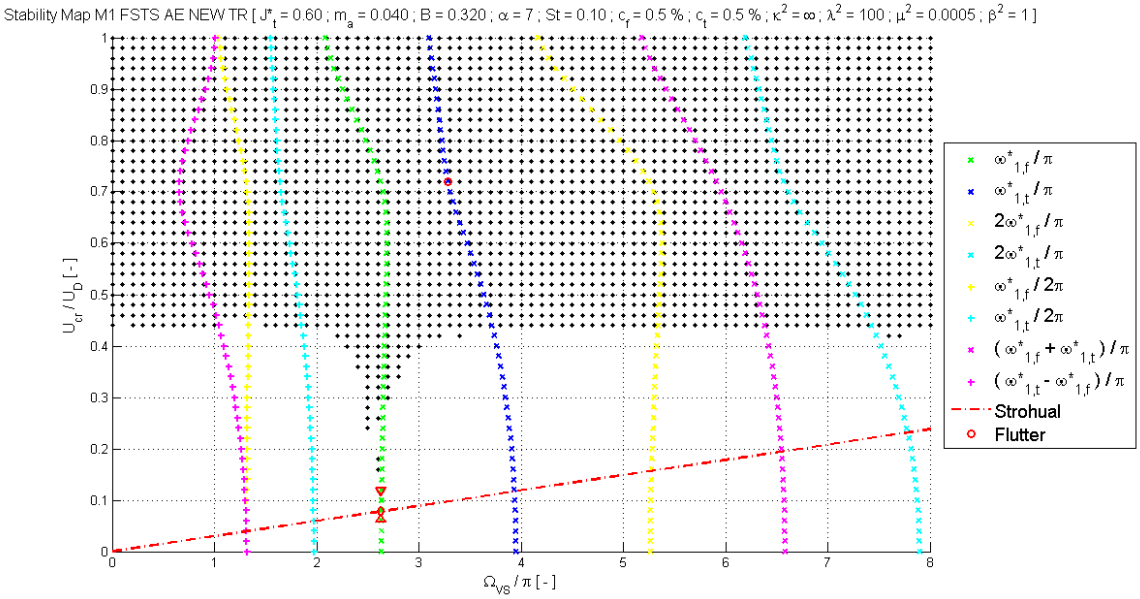

Figure 12: Stability map of the Aeroelastic model for slender deck section.

Even though the unstable region is more merged than in the pure structural model, we still recognize the main resonances, that are the linear primary and the 2:1 internal ones. The presence of wind not only obscures the stability maps but it also reduces (increases) the critical wind speed required to reach the torsional 2:1 internal (the flexural 1:1 external) resonances. In fact, as we can see the flutter instability is of torsional type.
An interesting feature is that near the curve of anti-resonance we get always a larger stable region. In fact, as reported also in different papers [41], the so called anti-parametric resonance with respect to the parametric and additive parametric ones has a stabilizing effect on the dynamic response of the system. This is due primary to the fact that this phenomenon is able to increase significantly the damping of the system. This particular property can be exploited trying to find the optimal geometrical and mechanical parameters able to maximize this intrinsic damping effect. The physical explanation of this feature hides behind the fact that as parametric excitation occur there is energy transfer between the two main interacting modes. Consequently, since higher order modes are characterized by higher damping ratios, then the system is able to dissipate faster that energy with respect to the system without Parametric excitation. Notice that we are dealing with an energetic exchange; hence, being the energy transfer not unidirectional, we should observe modulated vibrations time histories.
As we can see, as long as the deck is slender enough vortex sheeding is not sufficient to bring the structure to unstable conditions, while as the deck sectional aspect ratio reduces, Figure 13, the dynamic response diverges as the wind speed reaches levels that are much lower than those expected by the only flutter analysis.

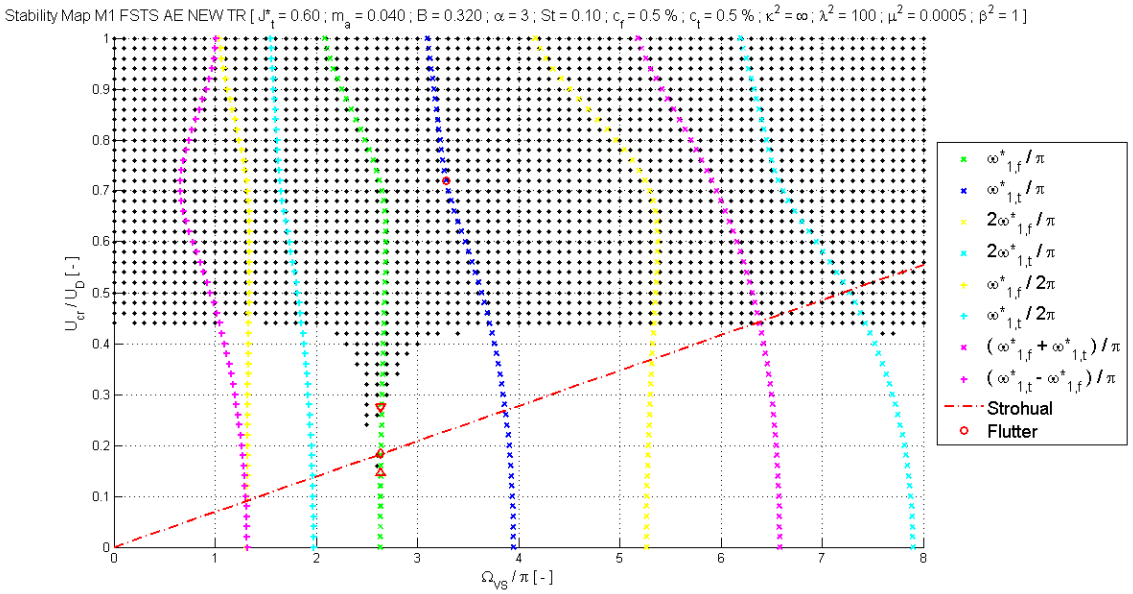

Figure 13: Stability map of the Aeroelastic model for bluff deck section.

Now we are able to comment the previous information in terms of flexural antinodal displacements by means the singles degree of freedom oscillator formulation. In fact, once we define the wind speed and the shedding frequency we know respectively the forcing term Γ_0 and the complex dynamic amplification factor $H(\delta)$. Considering Figure 14, we recognize immediately the usual shape characterizing every SDOF forced oscillator. We must remind that the equivalent oscillator is much more damped in the Aeroelastic model. Nevertheless, the total damping is never high enough to limit flexural oscillations to be lower than the cable's initial sag.

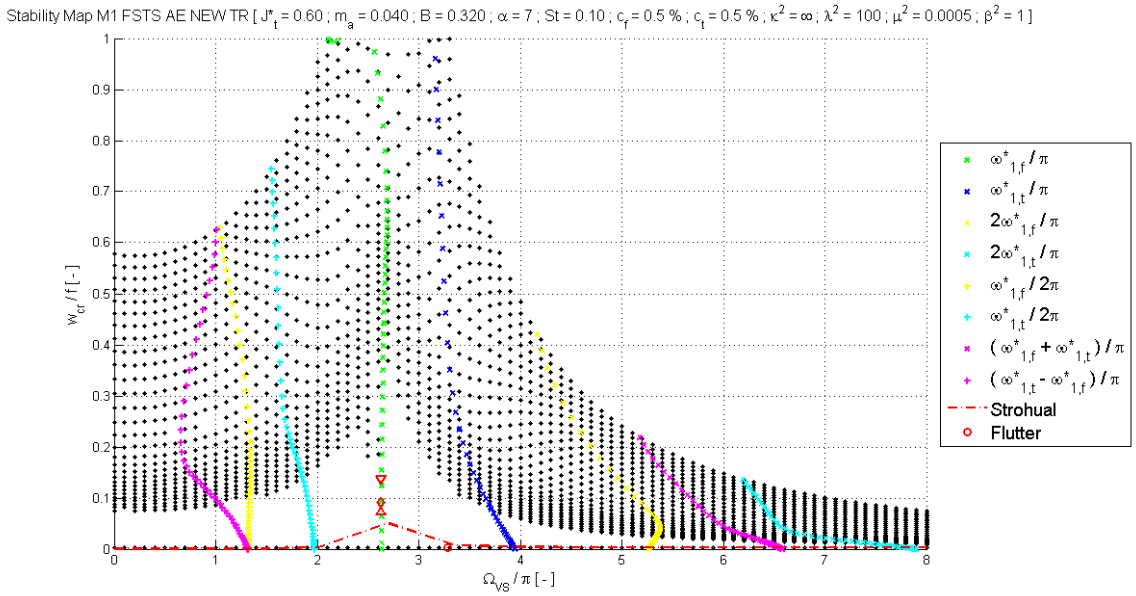

Figure 14 Unstable antinodal displacements of the Aeroelastic model for slender deck section.

Concerning the results related to bluff decks' section, for which unstable conditions are feasible, it is better to focus the attention on amplitudes that ranges up to $0.1 \cdot f$ (Figure 15).
First, it is worth noting that we have a lower bound representing the flexural motion in correspondence of torsional flutter instability for the Aeroelastic model. Second, it is important to underline that, according to Strouhal linear law, only in correspondence of 2:1 internal resonances the unstable conditions are feasible: in fact, all the other situations require too much high antinodal displacements that are difficult to observe in real life situations. Notice that the critical amplitudes so obtained are small enough to fulfil approximately the empirical limit threshold $z_{max} = 0.2 \cdot D/f \cong 0.009$ reminding us that vortex-shedding is a self-limiting phenomenon.

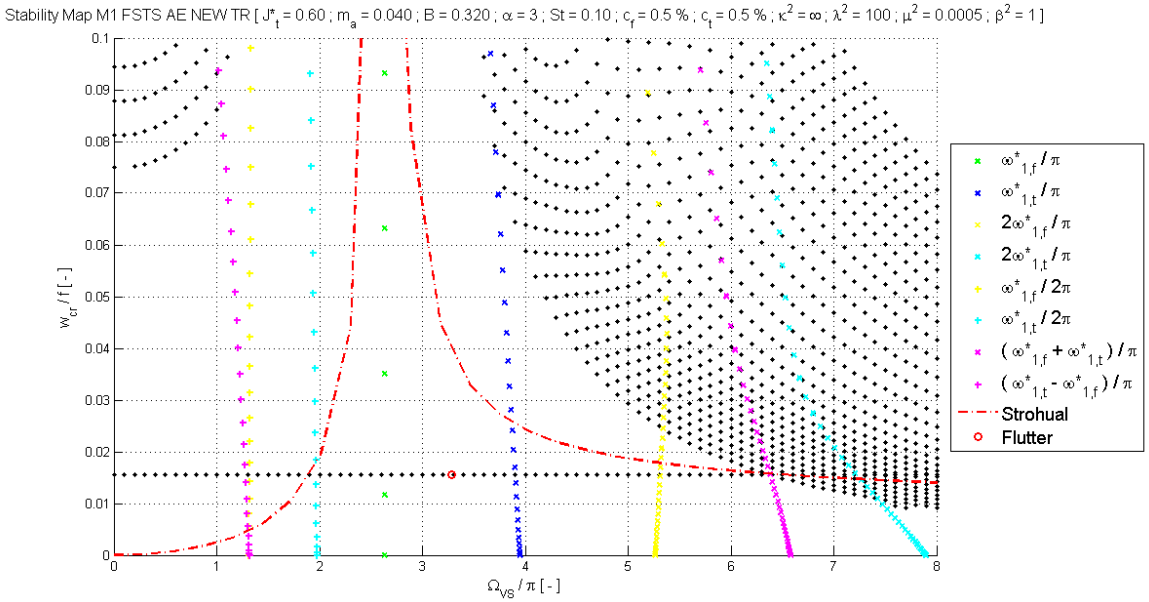

Figure 15 Unstable antinodal displacements of the Aeroelastic model for bluff deck section.

5 CONCLUSIONS

In this paper, a non-linear dynamic model of a suspension bridge is devised, with the purpose of providing a unified framework for the study of aeroelastic and internal parametric resonance instabilities.
Following the classical Deflection Theory, it has been possible to write the nonlinear static flexural response of a suspension bridge. The next step has consisted in the generalization of the displacement field in order to account for the torsional response of the deck-cables system. A deep insight in analytical aerodynamic field paves the way for the study of aeroelastic effects. Wind forces introduce additional mass, damping and stiffness that not only couples the linear equations of motion but also led the system to be no more self-adjoint. In fact, it loses its symmetries both in damping and stiffness matrices, making the structure susceptible respectively to flutter instabilities and static divergence problems.
The non-linear system has been treated in the framework of Floquet stability theory, thus achieving the stability maps in terms of wind speed and frequency of vortex shedding. After a thorough examination of the achieved results, we can conclude saying that parametric resonance is a critical phenomenon that can be activated by vortex-shedding as far as the sectional shape factor is low enough. This should warn very much engineers, since a phenomenon like vortex-shedding is usually taken in consideration just concerning serviceability limit states. On the contrary, we have just found that under certain conditions such a phenomenon may lead to very strong and critical unstable conditions in correspondence of wind speed that can be considered safe with respect to classical static divergence or dynamic flutter instabilities.
The present study can be improved by considering the possible slackening of vertical hangers, which may introduce an additional non-linearity to the system. In fact, the structural model considered herein is based on perfectly bilateral behavior of hangers, so that the deck displacement parameters are univocally connected to the cable displacements. In the presence of large upward displacement, slackening may occur, thus leading to a loss of stiffness for the whole system. In spite of this limitation, the model still provides valid results: in fact, view that the first modes are considered only, the unstable behavior corresponds to small displacements, see Figure 15. In the future development of this work, when dealing with higher modes, it will be unavoidable to introduce the loss of stiffness due to slackening.

REFERENCES

[1] A. Pugsley, *The theory of suspension bridges*. 2nd ed. Edward Arnold, 1968.

[2] D.B. Steinman, *A practical treatise on suspension bridges*. Wiley, 1953.

[3] F. Bleich, C. Mccullogh, R. Rosecrans, G. Vincent, *The mathematical theory of vibration in suspension bridges*, U.S. Government Printing Office, 1950.

[4] D. B. Steinman, A generalized deflection theory for suspension bridges, *Transaction of ASCE,* **100**, 1133-1234, 1935.

[5] J. Luco, J. Turmo, Linear vertical vibrations of suspension bridges: A review of continuum models and some new results, *Soil Dynamics and Earthquake Engineering*, **30**, 769–781, 2010.

[6] H. Irvine, *Cable structures*, MITpress, 1981.

[7] A. M. Abdel-Ghaffar, Vertical vibration analysis of suspension bridges, *ASCE Journal of Structural Division*, 106, 2053-2075, 1980.

[8] A. M. Abdel-Ghaffar, Free torsional vibrations of suspension bridges, *ASCE Journal of Structural Division*, 105, 767–788, 1979.

[9] A. M. Abdel-Ghaffar, Free lateral vibrations of suspension bridges, *ASCE Journal of Structural Division*, 104, 503-525, 1978.

[10] A. M. Abdel-Ghaffar, Suspension bridge vibration: continuum formulation, *ASCE Journal of the Engineering Mechanics Division*, 108, 1215–1232, 1982.

[11] A.M. Abdel-Ghaffar, L. Rubin, Nonlinear free vibrations of suspension bridges: Theory, *Journal of Engineering Mechanics*, 109, 313–329, 1983.

[12] A.M. Abdel-Ghaffar, L. Rubin, Nonlinear free vibrations of suspension bridges: Application, *Journal of Engineering Mechanics*, 109, 330–345, 1983.

[13] O.H. Ammann, T. Von Kármán, G.B. Woodruff, The failure of the Tacoma Narrows Bridge : a report to the honorable John M. Carmody, Federal Works Agency, 1941.

[14] R. L. Bisplinghoff, H. Ashley, R. L. Halfman, *Aeroelasticity*, Addison-Wesley, 1955.

[15] T. Theodorsen, General theory of aerodynamic instability and the mechanism of flutter, NACA Report n. 496, 1979.

[16] L. Salvatori, C. Borri, Frequency- and time-domain methods for the numerical modeling of full-bridge aeroelasticity, *Computers and Structures*, 85, 675-687, 2007.

[17] A. Arena, W. Lacarbonara, Nonlinear parametric modeling of suspension bridges under aeroelastic forces: torsional divergence and flutter, *Nonlinear Dynamics*, **70**, 2487-2510, 2012.

[18] D. Sado, Energy transfer in two-degree-of-freedom vibrating system : a survey, *Journal of Theoretical and Applied Mechanics*, 31, 151-173, 1993.

[19] Y. A. Rossikhin, M. V. Shitikova, Analysis of nonlinear free vibrations of suspension bridges, *Journal of Sound and Vibration*, 186, 369-393, 1995.

[20] M. Cevik, M. Pakdemirli, Non linear vibrations of suspension bridges with external excitation, *International Journal of Nonlinear Mechanics*, 40, 901-923, 2005.

[21] A. H. Nayfeh, Introduction to perturbation techniques, Wiley, 1993.

[22] G. Airoli, F. Gazzola, A new mathematical explanation of what triggered the catastrophic torsional mode of the Tacoma Narrows Bridge, *Applied Mathematical Modelling*, 39, 901-912, 2015.

[23] K. S. Moore, Large torsional oscillations in a suspension bridge: Multiple periodic solutions to a nonlinear wave equation, *SIAM Journal on Mathematical Analysis*, 33, 1411-1429, 2002.

[24] P.J. McKenna, Large torsional oscillations in suspension bridges revised: Fixing an old approximation, *American Mathematics Monthly*, 106, 1-18, 1999.

[25] D. Jacover, P. J. McKenna, Nonlinear torsional flexing in a periodically forced suspended beam, *Journal of Computational and Applied Mathematics*, 52, 241-265, 1994.

[26] R.H. Plaut, Snap loads and torsional oscillations of the original Tacoma Narrows Bridge, *Journal of Sound and Vibration*, 309, 613–636, 2008.

[27] R.H. Plaut, F.M. Davis, Sudden lateral asymmetry and torsional oscillations of section models of suspension bridges, *Journal of Sound and Vibration* 307, 2007, 894–905, 2007

[28] L. Cesari, Asymptotic behaviour and stability problems in ordinary differential equations, Springer, 1971.

[29] G. Herrmann, W. Hauger, On the interrelation of divergence, flutter and auto-parametric resonance, *Ingeneur-Archiv*, 42, 81-88, 1973.

[30] E. Simiu, R.H. Scanlan, *Wind effects on structures*, Wiley, 1996.

[31] J. M. W. Brownjohn, F. Magalhaes, E. Caetano, A. Cunha, Ambient vibration re-testing and operational modal analysis of the Humber Bridge, *Engineering Structures*, 32, 2003-2018, 2010.

[32] F. Nieto, S. Hernandez, J. A. Jurado, A. Mosquera, Analytical approach to sensitivity analysis of flutter speed in bridges considering deck mass, *Advances in Engineering Software*, 42, 117-129, 2011.

[33] S. Adnur, M. Gunaydin, A. C. Altunisik, B. Sevim, Construction stage analysis of Humber suspension bridge, *Applied Mathematical Modelling*, 36, 5492-5505, 2012.

[34] K. Kaptan, S. Tezacn, S. Altin, S. Cherry, Dynamic analysis of suspension bridges and full scale testing, *Procedia Engineering*, 14, 1065-1070, 2011.

[35] N. M. Apaydin, Earthquake performance assessment and retrofit investigations of two suspension bridges in Instanbul, *Soil Dynamics and Earthquake Engineering*, 30, 702-710, 2010.

[36] F. Ubertini, Effects of cables damage on vertical and torsional eigenproperties of suspension bridges, *Journal of Sound and Vibrations*, 333, 2404-2421, 2014.

[37] H. Wang, T. Tao, R. Zhou, X. Hua, A. Kareem, Parameter sensitivity study on flutter stability of long-span triple-tower suspension bridge, *Journal of Wind Engineering and Industrial Aerodynamics*, 128, 12-21, 2014.

[38] D. Cobo del Arco, A. C. Aparicio, Preliminary static analysis of suspension bridges, *Engineering Structures*, 23, 1096-1103, 2001.

[39] R. Karoumi, Some modelling aspects in the nonlinear finite element analysis of cable supported bridges, *Computer and Structures*, 71, 397-412, 1999.

[40] J. Malik, Sudden lateral asymmetric and torsional oscillations in the original Tacoma suspension bridge, *Journal of Sound and Vibration*, 332, 3772-3789, 2013.

[41] J. Welte, T. Kniffka, H. Ecker, Parametric excitation in a two degree of freedom MEMS system, *Shock and Vibrations*, 20, 1113-1124, 2013.

[42] S. Deniz, T. Staubli, Oscillating rectangular and octagonal profiles: interaction of leading- and trailing-edge vortex formation, *Journal of Fluids and Structures*, 11, 3–31, 1997.

[43] A. Larsen, J. H. Walther, Discrete vortex simulation of flow around five generic bridge deck sections, *Journal of Wind Engineering and Industrial Aerodynamics*, 77-78, 591-602, 1998.